

28. Charo IF, Ransohoff RM (2006) The many roles of chemokines and chemokine receptors in inflammation. *N Engl J Med* 354: 610–621
29. Sun X, Cheng G, Hao M et al (2010) CXCL12/CXCR4/CXCR7 chemokine axis and cancer progression. *Cancer Metastasis Rev* 29:709–722. Erratum 2011;30:269–270
30. Kawada K, Hosogi H, Sonoshita M et al (2007) Chemokine receptor CXCR3 promotes colon cancer metastasis to lymph nodes. *Oncogene* 26:4679–4688
31. Speetjens FM, Kuppen PJ, Sandel MH et al (2008) Disrupted expression of CXCL5 in colorectal cancer is associated with rapid tumor formation in rats and poor prognosis in patients. *Clin Cancer Res* 14:2276–2284
32. Zeelenberg IS, Ruuls-Van Stalle L, Roos E (2003) The chemokine receptor CXCR4 is required for outgrowth of colon carcinoma micrometastases. *Cancer Res* 63:3833–3839
33. Onoue T, Uchida D, Begum NM et al (2006) Epithelial-mesenchymal transition induced by the stromal cell-derived factor-1/CXCR4 system in oral squamous cell carcinoma cells. *Int J Oncol* 29:1133–1138
34. Taki M, Higashikawa K, Yoneda S et al (2008) Up-regulation of stromal cell-derived factor-1 α and its receptor CXCR4 expression accompanied with epithelial-mesenchymal transition in human oral squamous cell carcinoma. *Oncol Rep* 19:993–998
35. Fukunaga S, Maeda K, Noda E et al (2006) Association between expression of vascular endothelial growth factor C, chemokine receptor CXCR4 and lymph node metastasis in colorectal cancer. *Oncology* 71:204–211
36. Woo SU, Bae JW, Kim CH et al (2008) A significant correlation between nuclear CXCR4 expression and axillary lymph node metastasis in hormonal receptor negative breast cancer. *Ann Surg Oncol* 15:281–285
37. Su L, Zhang J, Xu H et al (2005) Differential expression of CXCR4 is associated with the metastatic potential of human non-small cell lung cancer cells. *Clin Cancer Res* 11:8273–8280
38. Speetjens FM, Liefers GJ, Korbee CJ et al (2009) Nuclear localization of CXCR4 determines prognosis for colorectal cancer patients. *Cancer Microenviron* 2:1–7
39. Na IK, Scheibenbogen C, Adam C et al (2008) Nuclear expression of CXCR4 in tumor cells of non-small cell lung cancer is correlated with lymph node metastasis. *Hum Pathol* 39:1751–1755
40. Lin SY, Makino K, Xia W et al (2001) Nuclear localization of EGF receptor and its potential new role as a transcription factor. *Nat Cell Biol* 3:802–808
41. Huang YC, Hsiao YC, Chen YJ et al (2007) Stromal cell-derived factor-1 enhances motility and integrin up-regulation through CXCR4, ERK and NF- κ B-dependent pathway in human lung cancer cells. *Biochem Pharmacol* 74:1702–1712
42. Burger M, Glodek A, Hartmann T et al (2003) Functional expression of CXCR4 (CD184) on small-cell lung cancer cells mediates migration, integrin activation, and adhesion to stromal cells. *Oncogene* 22:8093–8101
43. Futahashi Y, Komano J, Urano E et al (2007) Separate elements are required for ligand-dependent and -independent internalization of metastatic potentiator CXCR4. *Cancer Sci* 98:373–379
44. Shim H, Lau SK, Devi S et al (2006) Lower expression of CXCR4 in lymph node metastases than in primary breast cancers: potential regulation by ligand-dependent degradation and HIF-1 α . *Biochem Biophys Res Commun* 346:252–258
45. Kim SY, Lee CH, Midura BV et al (2008) Inhibition of the CXCR4/CXCL12 chemokine pathway reduces the development of murine pulmonary metastases. *Clin Exp Metastasis* 25:201–211
46. Horst D, Kriegl L, Engel J et al (2008) CD133 expression is an independent prognostic marker for low survival in colorectal cancer. *Br J Cancer* 99:1285–1289
47. Hong F, Tuyama A, Lee TF et al (2009) Hepatic stellate cells express functional CXCR4: role in stromal cell-derived factor-1 α -mediated stellate cell activation. *Hepatology* 49:2055–2067

LIVER, PANCREAS, AND BILIARY TRACT

Use of F-18 Fluorodeoxyglucose Positron Emission Tomography With Dual-Phase Imaging to Identify Intraductal Papillary Mucinous Neoplasm

MASAYOSHI SAITO,* TAKESHI ISHIHARA,* MOTOHISA TADA,* TOSHIO TSUYUGUCHI,* RINTARO MIKATA,* YUJI SAKAI,* KATSUNOBU TAWADA,* HARUTOSHI SUGIYAMA,* JO KUROSAWA,* MASAYUKI OTSUKA,† YOSHITAKA UCHIDA,§ KATSUHIRO UCHIYAMA,§ MASARU MIYAZAKI,‡ and OSAMU YOKOSUKA*

*Department of Medicine and Clinical Oncology, and †Department of General Surgery, Graduate School of Medicine, Chiba University; and §PET Diagnostic Imaging Center, Sannou Hospital Medical Center, Chiba, Japan

BACKGROUND & AIMS: We investigated the usefulness of dual-phase F-18 fluorodeoxyglucose positron emission tomography with computed tomography (FDG-PET/CT) to differentiate benign from malignant intraductal papillary mucinous neoplasms (IPMNs) and to evaluate branch-duct IPMNs.

METHODS: We used FDG-PET/CT to evaluate IPMNs in 48 consecutive patients who underwent surgical resection from May 2004 to March 2012. IPMNs were classified as benign (n = 16) or malignant (n = 32) on the basis of histology analysis. The ability of FDG-PET/CT to identify branch-duct IPMNs was compared with that of the International Consensus Guidelines.

RESULTS: The maximum standardized uptake value (SUVmax) was higher for early-phase malignant IPMNs than that for benign IPMNs (3.5 ± 2.2 vs 1.5 ± 0.4 , $P < .001$). When the SUVmax cutoff value was set at 2.0, early-phase malignant IPMNs were identified with 88% sensitivity, specificity, and accuracy. The retention index values for malignant and benign IPMNs were 19.6 ± 17.8 and -2.6 ± 12.9 , respectively. When the SUVmax cutoff was set to 2.0 and the retention index value to -10.0 , early-phase malignant IPMNs were identified with 88% sensitivity, 94% specificity, and 90% accuracy. In identification of branch-duct IPMNs, when the SUVmax cutoff was set to 2.0, the sensitivity, specificity, and accuracy values were 79%, 92%, and 84%, respectively. By using a maximum main pancreatic duct diameter ≥ 7 mm, the Guidelines identified branch-duct IPMNs with greater specificity than FDG-PET/CT. The Guidelines criteria of maximum cyst size ≥ 30 mm and the presence of intramural nodules identified branch-duct IPMNs with almost equal sensitivity to FDG-PET/CT. **CONCLUSIONS:** Dual-phase FDG-PET/CT is useful for preoperative identification of malignant IPMN and for evaluating branch-duct IPMN.

Keywords: Imaging; Diagnosis; Comparison; Pancreas; Carcinoma.

Since its first description by Ohashi et al¹ in 1982, the reported incidence of intraductal papillary mucinous neoplasm (IPMN) has been increasing because of improvements in imaging modalities and growing clinical awareness. IPMN is defined as an intraductal tumor formed of papillary proliferations of pancreatic mucin-producing epithelial cells.² IPMN manifests in a variety of histologic grades, is associated with the adenoma-carcinoma sequence, and may be benign or malignant.³ The frequency of malignancy differs according to type of IPMN. The risk of malignancy in main-duct type IPMN is

57%–92%,^{4–6} as compared with branch-duct type IPMN, in which the risk of malignancy ranges from 6% to 46%.^{7–9} Because of the poor prognosis of invasive carcinoma,¹⁰ tumor resection is the only curative treatment for malignant IPMN. However, preoperative determination of malignant IPMN remains difficult, even with different imaging techniques.

In 2004, the International Association of Pancreatology outlined International Consensus Guidelines (ICG) for the management of IPMN.¹¹ The ICG recommends surgical resection in all cases of main-duct type IPMN. Because of the low malignant potential of branch-duct type IPMN, the ICG recommends surgical resection in the presence of 1 or more of the following clinical indicators: (1) cyst-related symptoms, (2) main pancreatic duct (MPD) diameter ≥ 7 mm, (3) cyst size ≥ 30 mm, (4) presence of intramural nodules, and (5) cyst fluid cytology suspicious/positive for malignancy. However, proper treatment strategy for branch type IPMN has not been well established.

Characterization of IPMN is accomplished by using several imaging modalities such as multidetector row computed tomography, magnetic resonance cholangiopancreatography (MRCP), and endoscopic ultrasonography (EUS). F-18 fluorodeoxyglucose positron emission tomography/computed tomography (FDG-PET/CT) has been widely used in the evaluation of various malignancies. FDG-PET/CT is a functional and anatomic imaging modality that detects abnormalities in glucose metabolism by using a glucose analogue combined with anatomic correlation. However, use of FDG-PET/CT in the evaluation of malignant IPMN has been limited.^{12–15} Because FDG is not a tumor-specific substance, it accumulates in inflammatory lesions, which can cause false-positive results.¹⁶ To solve this problem, some investigators^{17–19} performed dual-phase FDG-PET imaging, which includes delayed-phase imaging to differentiate benign from malignant lesions in various cancers. However, the useful-

Abbreviations used in this paper: EUS, endoscopic ultrasonography; FDG-PET/CT, F-18 fluorodeoxyglucose positron emission tomography/computed tomography; HGD, high-grade dysplasia; ICG, International Consensus Guidelines; IGD, intermediate-grade dysplasia; IPMN, intraductal papillary mucinous neoplasm; LGD, low-grade dysplasia; MPD, main pancreatic duct; MRCP, magnetic resonance cholangiopancreatography; RI, retention index; SUVmax, maximum standardized uptake value.

© 2013 by the AGA Institute
1542-3565/\$36.00

<http://dx.doi.org/10.1016/j.cgh.2012.10.037>

ness of dual-phase imaging in differentiating between benign and malignant IPMNs has not been previously examined.

The primary objective of the current study was to evaluate the usefulness of FDG-PET/CT in differentiating between histologically confirmed benign and malignant IPMNs. The efficacy of dual-phase imaging was also examined. In addition, the usefulness of FDG-PET/CT in branch-duct type IPMN was compared with evaluation that is based on clinical features that indicate malignant potential according to the ICG.

Materials and Methods

Patients

Between May 2004 and March 2012, FDG-PET/CT was used in the evaluation of 48 consecutive patients with IPMN in whom tumors were surgically resected at our institute. Final pathologic diagnoses were obtained by pathologic review of the surgical specimens and confirmed on the basis of the World Health Organization classification.²⁰ In this study, medical records of these 48 histologically confirmed cases of IPMN were analyzed retrospectively.

In all patients, sex, age, serum carcinoembryonic antigen levels, serum carbohydrate antigen 19-9 levels, tumor location, type of IPMN, MPD diameter, cyst size, presence and height of intramural nodules, and maximum standardized uptake value (SUVmax) in the early phase were investigated. In 18 patients, SUVmax in the delayed phase was also investigated. Multidetector row computed tomography, EUS, and MRCP were performed for all patients. In 41 patients, pancreatic juice was sampled before surgical resection for cytologic examination. Diagnoses based on cytology were categorized into the following 5 groups: benign, reactive process, atypical cells indeterminate for malignancy, malignancy strongly suspected, and cytology conclusive for malignancy. Cytologic results in which malignancy was strongly suspected or conclusive were regarded as cancer positive, and atypical results were regarded as cancer negative. In this study, MPD diameter, cyst size, and presence and height of intramural nodules were measured by EUS. IPMN was classified into 2 types, main-duct type and branch-duct type, according to the location of the main lesion and on the basis of histologic features.

Surgical Indications

Surgical resection was performed in all cases of main-duct type IPMN and in cases of branch-duct type IPMN that met at least 1 of the following ICG criteria¹¹: cyst size ≥ 30 mm, MPD diameter ≥ 7 mm, presence of intramural nodules, or cytologically confirmed malignant and symptomatic IPMN. Types of surgery performed included pancreaticoduodenectomy (n = 23), distal pancreatectomy (n = 23), and pancreatectomy (n = 2).

Histopathologic Diagnosis

According to the World Health Organization classification,²⁰ IPMN was classified into low-grade dysplasia (LGD), intermediate-grade dysplasia (IGD), high-grade dysplasia (HGD), or invasive carcinoma. In this study, malignant IPMN was defined as HGD and invasive carcinoma, and benign IPMN was defined as LGD and IGD. Histopathologic analysis led to diagnoses of LGD in 14 patients, IGD in 2 patients, HGD in 17 patients, and invasive carcinoma in 15 patients.

F-18 Fluorodeoxyglucose Positron Emission Tomography/Computed Tomography Imaging

FDG-PET/CT was performed in Chiba University Hospital and Sannou Hospital. The PET scanners used were Aquiduo (Toshiba Medical Systems, Tokyo, Japan), Advance NXi (GE Healthcare, Waukesha, WI), and Discovery ST (GE Healthcare). All patients fasted for at least 5 hours before examination. Blood glucose was measured before injection of FDG. The injection dose was 4 MBq/kg depending on the patient's weight. Early-phase scans were performed 60 minutes after injection in all 48 patients. Dual-phase FDG-PET/CT scans were performed in the patients enrolled after April 2009. Delayed-phase scans were performed 120 minutes after injection in 18 patients. The reconstructed images were interpreted by physicians with many years of experience in nuclear medicine. FDG uptake was evaluated both visually and semiquantitatively by using SUVmax. SUVmax was defined as the highest pixel value related to the neoplasm burden in each study. It was computed by using the following formula: $SUVmax = \text{Maximum activity concentration in the neoplasm (kBq/mL)} / [\text{Injected dose (MBq)} / \text{Body weight (kg)}]$. The retention index (RI) was also defined by using the following formula: $(SUV_{\text{delayed}} - SUV_{\text{early}}) \times 100 / SUV_{\text{early}}$.

Statistical Analysis

Statistical differences between subgroups were determined by using the Mann-Whitney *U* test and the χ^2 test. The optimal cutoff value of SUVmax to differentiate benign from malignant IPMNs was determined by receiver operating characteristic analysis. Sensitivity, specificity, and accuracy were also calculated. All statistical analyses were performed by using SPSS software (SPSS version 20.0; SPSS, Inc, Chicago, IL). *P* values $< .05$ were considered to be statistically significant.

Results

Clinical characteristics of the 48 patients (32 men, 16 women; mean age, 68.6 ± 7.3 years; range, 51–82 years) included in this study are summarized in Table 1. On the basis of histopathologic analysis, benign IPMN was diagnosed in 16 patients and malignant IPMN in 32 patients.

The significant differences between benign and malignant IPMN cases are summarized in Table 1. No significant differences in sex, age, tumor location, tumor type, tumor markers, cyst size, or presence of intramural nodules were observed between the 2 groups. The mean MPD diameter in malignant IPMN cases was larger than that in benign IPMN cases (8.1 ± 4.0 mm vs 4.7 ± 2.2 mm, $P = .001$). The mean height of the intramural nodules was larger in malignant IPMN cases than that in benign IPMN cases (12.6 ± 6.2 mm vs 7.3 ± 4.7 mm, $P = .021$). In 41 patients, endoscopic retrograde cholangiopancreatography was performed for cytologic analysis of pancreatic juice before surgical resection. From these results, 8 patients (16.7%) were diagnosed with malignant IPMN.

The mean SUVmax in the early phase of IPMN in all 48 cases was 2.9 ± 2.0 (range, 1.0–12.3). The mean SUVmax in the early phase of malignant IPMN was significantly higher than that in benign IPMN cases (3.5 ± 2.2 vs 1.5 ± 0.4 , $P < .001$).

Figure 1 depicts correlations between histopathologic types of IPMN and SUVmax in the early phase. Mean SUVmax in the early phase of LGD and IGD, HGD, and invasive carcinoma

Table 1. Clinical Characteristics of 48 IPMN Patients

	Benign (n = 16)	Malignant (n = 32)	P value
Sex			.588 ^a
Male	12	20	
Female	4	12	
Age (y)	67.2 ± 7.9	69.3 ± 7.0	.424 ^b
Location			.919 ^a
Head	7	16	
Body + tail	9	16	
Type			.234 ^a
Main duct	3	13	
Branch duct	13	19	
Diameter of MPD (mm)	4.7 ± 2.2	8.1 ± 4.0	.001 ^b
Cyst size (mm)	27.3 ± 7.6	29.9 ± 20.4	.974 ^b
Intramural nodules			.421 ^a
Present	10	25	
Absent	6	7	
Height of intramural nodules (mm)	7.3 ± 4.7	12.6 ± 6.2	.021 ^b
Cytology of pancreatic juice (N = 41)			.466 ^a
Negative	11	22	
Positive	1	7	
Tumor marker			
Carcinoembryonic antigen (ng/mL)	3.4 ± 1.8	4.0 ± 3.3	.678 ^b
Carbohydrate antigen 19-9 (U/mL)	16.6 ± 16.6	43.0 ± 60.3	.167 ^b
SUVmax (early phase)	1.5 ± 0.4	3.5 ± 2.2	<.001 ^b

^aχ² test.

^bMann-Whitney U test.

were 1.5 ± 0.4, 2.6 ± 0.9, and 4.6 ± 2.7, respectively. The mean SUVmax in the early phase of HGD cases was significantly higher than that of LGD and IGD (*P* < .001). The mean SUVmax in the early phase of invasive carcinoma was also higher than that in HGD cases (*P* < .001).

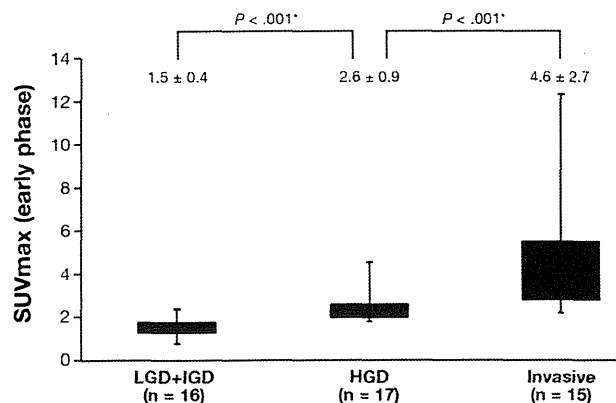


Figure 1. Correlation between pathologic type IPMN and SUVmax in the early phase. The SUVmax on early phase of LGD and IGD, HGD, and invasive carcinoma was 1.5 ± 0.4, 2.6 ± 0.9, and 4.6 ± 2.7, respectively. The SUVmax of HGD was statistically higher than those of LGD and IGD (*P* < .001). The SUVmax of invasive carcinoma was also higher than that of HGD (*P* < .001). *Mann-Whitney U test.

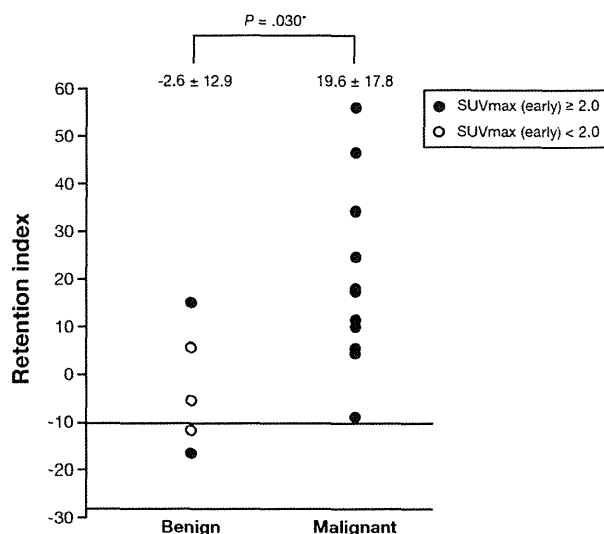


Figure 2. Results for 18 patients in whom dual-phase FDG-PET/CT was performed. Twelve of 13 malignant IPMNs (92.3%) had further increase in SUVmax; 3 of 5 benign IPMNs (60.0%) had decrease in SUVmax on delayed phase. The RI of malignant and benign IPMNs was 19.6 ± 17.8 and -2.6 ± 12.9 (*P* = .030). If a combination of the SUVmax cutoff value of 2.0 in the early phase and the RI value of -10.0 for detection of malignant IPMN was used, one false-positive adenoma case (SUVmax: early 2.4, delayed 2.0) may be diagnosed as benign IPMN. *Mann-Whitney U test.

In this study, dual-phase FDG-PET/CT was performed in 18 patients. Histopathologic analysis identified LGD and IGD in 5 of these patients, HGD in 4, and invasive carcinoma in 9. Figure 2 shows RI values for these 18 patients. In 12 of the 13 cases of malignant IPMN (92.3%), SUVmax increased further in the delayed phase, whereas in 3 of 5 cases of benign IPMN (60.0%), SUVmax decreased in the delayed phase. RI values in malignant and benign IPMNs were 19.6 ± 17.8 and -2.6 ± 12.9, respectively. Differences between the 2 groups were statistically significant (*P* = .030).

Table 2 displays values for the sensitivity, specificity, and accuracy of FDG-PET/CT from the receiver operating characteristic analysis of malignant IPMN cases. When the cutoff value of SUVmax in the early phase was set to 2.0, the sensitivity, specificity, and accuracy in malignant IPMN cases were all 88%. When the cutoff value of SUVmax in the early phase was set to 2.0 and the RI value was set at -10.0, the sensitivity, specificity, and accuracy of FDG-PET/CT in malignant IPMN cases improved to 88%, 94%, and 90%, respectively.

The usefulness of FDG-PET/CT in evaluation of branch-duct type IPMN was compared with that of evaluation according to the clinical features indicating malignant potential in IPMN, as outlined by the ICG (Table 3). In cases with branch-duct type IPMN, when the cutoff value of SUVmax in the early phase was set to 2.0, the sensitivity, specificity, and accuracy of FDG-PET/CT in identifying malignant IPMN cases were 79%, 92%, and 84%, respectively. By using the criteria of maximum MPD diameter ≥ 7 mm and cytologic analysis of pancreatic juice, specificity was superior to that of FDG-PET/CT, but sensitivity and accuracy were inferior to those of FDG-PET/CT. On the other hand, by using the criteria of maximum cyst size ≥ 30 mm and the presence of intramural nodules, sensitivity

Table 2. Diagnosis by Using SUVmax (Early Phase) Alone and Combination of SUVmax (Early Phase) and RI for Detection of Malignant IPMNs

FDG-PET/CT diagnosis	Final diagnosis		
	Benign	Malignant	
	LGD + IGD	HGD	Invasive
Cutoff value: 2.0 for SUVmax in early phase			
Positive	2	13	15
Negative	14	4	0
Sensitivity (%)			88
Specificity (%)			88
Accuracy (%)			88
Cutoff value: 2.0 for SUVmax in early phase and -10.0 for RI			
Positive	1	13	15
Negative	15	4	0
Sensitivity (%)			88
Specificity (%)			94
Accuracy (%)			90

was almost equal to that of FDG-PET/CT, but specificity and accuracy were inferior to those of FDG-PET/CT.

Discussion

In this study, the preoperative usefulness of FDG-PET/CT in differentiating between histologically confirmed benign and malignant IPMNs was evaluated. When the cutoff value for SUVmax in the early phase was set to 2.0, the sensitivity, specificity, and accuracy in identifying malignant IPMN cases were all high (88%). Several other studies have also demonstrated the usefulness of FDG-PET/CT in detecting malig-

nant IPMN. Sperti et al¹² reported sensitivity, specificity, and accuracy levels of 92%, 97%, and 95%, respectively, at a cutoff level of 2.5 in 64 patients with IPMN. Tomimaru et al¹³ examined several cutoff levels in 29 cases of IPMN. The sensitivity, specificity, and accuracy levels in that study were 93%, 100%, and 96%, respectively, at a cutoff level of 2.5 and 93%, 86%, and 89%, respectively, at a cutoff level of 2.0.

In the current study, the optimal cutoff value was set at 2.0, slightly lower than that used in previous studies. On the basis of the results of this study and those of previous studies, a cutoff value between 2.0 and 2.5 may be optimal. The cutoff value was low in this study because of the higher number of patients diagnosed as HGD than were diagnosed with invasive carcinoma in the group of patients with malignant IPMN. In the report of Sperti et al,¹² 21 of 26 malignant IPMN cases were diagnosed with invasive carcinoma. In the report of Tomimaru et al,¹³ 11 of 14 malignant IPMN cases were diagnosed with invasive carcinoma. Therefore, the incidence of invasive carcinoma was higher in those studies than in the present study.

FDG-PET/CT has been widely used in the evaluation of various malignant lesions, but high SUVmax may also be found in various benign conditions evaluated by using this modality because FDG is not a tumor-specific substance. FDG also accumulates in inflammatory lesions, which can cause false-positive results.¹⁶ Dual-phase FDG-PET/CT has been performed in some studies¹⁷⁻¹⁹ to differentiate benign from malignant lesions in various cancers. The longer time required for levels of FDG to plateau in cancer cells than in inflammatory cells may be related to the up-regulation of glucose consumption demonstrated in malignant cells to obtain more energy for proliferation. This leads to graded concentrations of FDG in tumor cells. In contrast, a prolonged period of FDG uptake is less common in inflammatory lesions or normal tissues.¹⁹ Potential limitations of dual-phase FDG-PET/CT include its low availability, high exposure to radiation, and increased procedural time.

Table 3. Usefulness of FDG-PET/CT in Evaluation of Branch-Duct Type IPMN Compared With That of Evaluation According to Clinical Features Indicating Malignant Potential in IPMN, as Outlined by the ICG

Clinical parameters	Final diagnosis			Sensitivity (%)	Specificity (%)	Accuracy (%)
	Benign	Malignant				
	LGD + IGD	HGD	Invasive			
FDG-PET/CT cutoff value: 2.0 for SUVmax in early phase						
Positive	1	8	7	79	92	84
Negative	12	4	0			
Diameter of MPD (mm)						
≥ 7	0	5	4	47	100	69
< 7	13	7	3			
Cyst size (mm)						
≥ 30	9	9	6	79	31	59
< 30	4	3	1			
Intramural nodules						
Present	8	11	5	84	38	66
Absent	5	1	2			
Cytology of pancreatic juice (N = 26)						
Positive	0	1	1	13	100	46
Negative	10	9	5			

In pancreatic diseases, Nakamoto *et al*²¹ suggested that dual-phase FDG-PET/CT may be a reliable method of differentiating pancreatic cancer from chronic pancreatitis. Okano *et al*²² indicated that dual-phase FDG-PET/CT is a useful modality for detection of small pancreatic cancers. However, the usefulness of dual-phase FDG-PET imaging in differentiation between benign and malignant IPMNs was not examined in other studies. IPMN shows a wide spectrum of histologic grades ranging from benign to malignant neoplasms. Benign IPMN is thought to be low in metabolic activity; therefore, we assumed SUVmax of benign IPMN to decrease in the delayed phase.

In this study, dual-phase FDG-PET/CT imaging was performed in 18 patients. RI values in malignant and benign IPMN cases were 19.6 ± 17.8 and -2.6 ± 12.9 , respectively, and a significant difference was observed between the 2 groups. Furthermore, in 12 of 13 malignant IPMN cases (92.3%), SUVmax increased further in the delayed phase, whereas in 3 of 5 benign IPMN cases (60.0%), SUVmax decreased in the delayed phase. If a combination of the SUVmax cutoff value of 2.0 in the early phase and the RI value of -10.0 for detection of malignant IPMN was used, one false-positive case of adenoma (SUVmax: early phase 2.4, delayed phase 2.0) may be diagnosed as benign IPMN. Specificity improved from 88% to 94%, and accuracy improved from 88% to 90%. Pancreatitis had been observed 1 month before FDG-PET/CT examination in this false-positive case; therefore, FDG accumulation in an inflammatory lesion may have been responsible for this false-positive finding. Thus, this 2-step method of FDG-PET/CT may be useful for differentiating between benign and malignant IPMNs.

The ICG recommends surgical resection for all cases of main-duct type IPMN. On the other hand, branch-duct type IPMN has low malignant potential. However, management of branch-duct type IPMN has not been well established. In this study, FDG-PET/CT achieved good sensitivity, specificity, and accuracy in branch-duct type IPMN (79%, 92%, and 84%, respectively). FDG-PET/CT was also useful in differentiating between benign and malignant disease in branch-duct type IPMN. The ICG recommends evaluation according to cyst size, MPD diameter, and the presence of intramural nodules in the tumor in determination of malignant potential in cases of IPMN. The validity of these recommendations for the detection of malignancy was retrospectively evaluated in 2 follow-up studies. Both studies found the ICG criteria to have a sensitivity of 100% in diagnosing malignancy. However, the specificity of the guidelines in diagnosing malignancy was only 23%–31%, resulting in a relatively high resection rate for those without malignancy.^{23,24}

In this study, the usefulness of FDG-PET/CT in detection of malignancy in branch-duct type IPMN was compared with detection that was based on these clinical features and EUS findings. EUS is a highly operator-dependent procedure, but several retrospective studies^{25,26} have demonstrated its accuracy in the diagnosis of IPMN. EUS has been used to detect intramural lesions in the pancreatic duct, with good results. Nakagawa *et al*²⁷ found EUS to be highly sensitive for intramural lesion detection in cases of IPMN, but the specificity of this modality was low, as indicated by the relatively high rate of false-positive cases in that study. These results were caused by mucin in the pancreatic duct, which may appear to be intramural lesions on EUS. In the current study, EUS was sufficiently sensitive in determination of cyst size ≥ 30 mm and the

presence of intramural nodules, but specificity and accuracy were inferior to those of FDG-PET/CT. On the other hand, EUS showed good specificity for MPD diameter ≥ 7 mm, but its sensitivity and accuracy were inferior to those of FDG-PET/CT. These results demonstrate the usefulness of FDG-PET/CT in branch-duct type IPMN compared with an evaluation that was based on clinical features suggesting malignant potential. In the current study, clinical features were measured on the basis of EUS findings, but MRCP also has been reported to be effective for evaluating the ICG criteria.²⁸ Baiocchi *et al*²⁹ suggested that a combination of MRCP and FDG-PET/CT would be optimal for branch-duct IPMN.

Suggestions for treatment strategies in cases of IPMN can be made on the basis of the results of the current study. Operative adaptations have been narrowed down according to the ICG criteria for IPMN; in these patients, if a combination of the SUVmax cutoff value of 2.0 in the early phase and the RI value of -10.0 in the FDG-PET/CT study was used, the diagnostic accuracy may be improved. Further studies on larger numbers of patients are necessary to confirm the reliability of this strategy.

Conclusions

FDG-PET/CT with dual-phase imaging is a useful clinical modality for preoperative determination of malignant IPMN. FDG-PET/CT is useful in the evaluation of branch-duct type IPMN compared with evaluation that is based on the clinical features suggesting malignant potential outlined in the ICG.

References

1. Ohhashi K, Murakami Y, Maruyama M, *et al*. Four cases of mucus-secreting pancreatic cancer. *Prog Dig Endosc* 1982;20:348–351.
2. Kloppel G, Solcia E, Longnecker DS, *et al*. Histological typing of tumors of the exocrine pancreas. In: World Health Organization: international histological classification of tumours. 2nd ed. Berlin, Germany: Springer, 1996:15–21.
3. Goh BK, Tan YM, Cheow PC, *et al*. Cystic neoplasms of the pancreas with mucin-production. *Eur J Surg Oncol* 2005;31:282–287.
4. Salvia R, Fernández-del Castillo C, Bassi C, *et al*. Main-duct intraductal papillary mucinous neoplasms of the pancreas: clinical predictors of malignancy and long-term survival following resection. *Ann Surg* 2004;239:678–685.
5. Sugiyama M, Izumisato Y, Abe N, *et al*. Predictive factors for malignancy in intraductal papillary-mucinous tumours of the pancreas. *Br J Surg* 2003;90:1244–1249.
6. Terris B, Ponsot P, Paye F, *et al*. Intraductal papillary mucinous tumors of the pancreas confined to secondary ducts show less aggressive pathologic features as compared with those involving the main pancreatic duct. *Am J Surg Pathol* 2000;24:1372–1377.
7. Sohn TA, Yeo CJ, Cameron JL, *et al*. Intraductal papillary mucinous neoplasms of the pancreas: an updated experience. *Ann Surg* 2004;239:788–797.
8. Kitagawa Y, Unger TA, Taylor S, *et al*. Mucus is a predictor of better prognosis and survival in patients with intraductal papillary mucinous tumor of the pancreas. *J Gastrointest Surg* 2003;7:12–19.
9. Matsumoto T, Aramaki M, Yada K, *et al*. Optimal management of the branch duct type intraductal papillary mucinous neoplasms of the pancreas. *J Clin Gastroenterol* 2003;36:261–265.

10. Yamao K, Ohashi K, Nakamura T, et al. The prognosis of intraductal papillary mucinous tumors of the pancreas. *Hepato-gastroenterology* 2000;47:1129–1134.
11. Tanaka M, Chari S, Adsay V, et al. International Consensus Guidelines for management of intraductal papillary mucinous neoplasms and mucinous cystic neoplasms of the pancreas. *Pancreatol* 2006;6:17–32.
12. Sperti C, Bissoli S, Pasquali C, et al. 18-Fluorodeoxyglucose positron emission tomography enhances computed tomography diagnosis of malignant intraductal papillary mucinous neoplasms of the pancreas. *Ann Surg* 2007;246:932–937.
13. Tomimaru Y, Takeda Y, Tatsumi M, et al. Utility of 2-[18F] fluoro-2-deoxy-D-glucose positron emission tomography in differential diagnosis of benign and malignant intraductal papillary-mucinous neoplasm of the pancreas. *Oncol Rep* 2010;24:613–620.
14. Takanami K, Hiraide T, Tsuda M, et al. Additional value of FDG PET/CT to contrast-enhanced CT in the differentiation between benign and malignant intraductal papillary mucinous neoplasms of the pancreas with mural nodules. *Ann Nucl Med* 2011;25:501–510.
15. Hong HS, Yun M, Cho A, et al. The utility of F-18 FDG PET/CT in the evaluation of pancreatic intraductal papillary mucinous neoplasm. *Clin Nucl Med* 2010;35:776–779.
16. Shreve PD. Focal fluorine-18 fluorodeoxyglucose accumulation in inflammatory pancreatic disease. *Eur J Nucl Med* 1998;25:259–264.
17. Matthies A, Hickeson M, Cuchiara A, et al. Dual time point 18F-FDG PET for the evaluation of pulmonary nodules. *J Nucl Med* 2002;43:871–875.
18. Kubota K, Itoh M, Ozaki K, et al. Advantage of delayed whole-body FDG-PET imaging for tumor detection. *Eur J Nucl Med* 2001;28:696–703.
19. Zhuang H, Pourdehnad M, Lambright ES, et al. Dual time point 18F-FDG PET imaging for differentiating malignant from inflammatory processes. *J Nucl Med* 2001;42:1412–1417.
20. Bosman FT, Carneiro F, Hruban RH, et al. WHO classification of tumours of the digestive system. Lyon, France: IARC Press, 2010.
21. Nakamoto Y, Higashi T, Sakahara H, et al. Delayed (18)F-fluoro-2-deoxy-D-glucose positron emission tomography scan for differentiation between malignant and benign lesions in the pancreas. *Cancer* 2000;89:2547–2554.
22. Okano K, Kakinoki K, Akamoto S, et al. 18F-fluorodeoxyglucose positron emission tomography in the diagnosis of small pancreatic cancer. *World J Gastroenterol* 2011;17:231–235.
23. Tang RS, Weinberg B, Dawson DW, et al. Evaluation of the guidelines for management of pancreatic branch-duct intraductal papillary mucinous neoplasm. *Clin Gastroenterol Hepatol* 2008;6:815–819.
24. Pelaez-Luna M, Chari ST, Smyrk TC, et al. Do consensus indications for resection in branch duct intraductal papillary mucinous neoplasm predict malignancy? A study of 147 patients. *Am J Gastroenterol* 2007;102:1759–1764.
25. Baba T, Yamaguchi T, Ishihara T, et al. Distinguishing benign from malignant intraductal papillary mucinous tumors of the pancreas by imaging techniques. *Pancreas* 2004;29:212–217.
26. Kubo H, Nakamura K, Itaba S, et al. Differential diagnosis of cystic tumors of the pancreas by endoscopic ultrasonography. *Endoscopy* 2009;41:684–689.
27. Nakagawa A, Yamaguchi T, Ohtsuka M, et al. Usefulness of multidetector computed tomography for detecting protruding lesions in intraductal papillary mucinous neoplasm of the pancreas in comparison with single-detector computed tomography and endoscopic ultrasonography. *Pancreas* 2009;38:131–136.
28. Guarise A, Faccioli N, Ferrari M, et al. Evaluation of serial changes of pancreatic branch duct intraductal papillary mucinous neoplasms by follow-up with magnetic resonance imaging. *Cancer Imaging* 2008;8:220–228.
29. Baiocchi GL, Portolani N, Bertagna F, et al. Possible additional value of 18FDG-PET in managing pancreas intraductal papillary mucinous neoplasms: preliminary results. *J Exp Clin Cancer Res* 2008;27:10.

Reprint requests

Address requests for reprints to: Masayoshi Saito, MD, Department of Medicine and Clinical Oncology, Graduate School of Medicine, Inohana 1-8-1, Chuo Ward, Chiba 260-8670, Japan. e-mail: sai_masa3110@yahoo.co.jp; fax: 81-43-226-2088.

Conflicts of interest

The authors disclose no conflicts.

Available online at www.sciencedirect.com

SciVerse ScienceDirect

journal homepage: www.JournalofSurgicalResearch.com

Akt/mTOR signaling pathway is crucial for gemcitabine resistance induced by Annexin II in pancreatic cancer cells

Shingo Kagawa, MD, PhD,^{a,b} Shigetsugu Takano, MD, PhD,^{a,b}
 Hideyuki Yoshitomi, MD, PhD,^{a,*} Fumio Kimura, MD, PhD,^a Mamoru Satoh, PhD,^b
 Hiroaki Shimizu, MD, PhD,^a Hiroyuki Yoshidome, MD, PhD,^a
 Masayuki Ohtsuka, MD, PhD,^a Atsushi Kato, MD, PhD,^a
 Katsunori Furukawa, MD, PhD,^a Kazuyuki Matsushita, MD, PhD,^b
 Fumio Nomura, MD, PhD,^b and Masaru Miyazaki, MD, PhD^a

^aDepartment of General Surgery, Graduate School of Medicine, Chiba University, Chiba, Japan

^bDepartment of Molecular Diagnosis, Graduate School of Medicine, Chiba University, Chiba, Japan

ARTICLE INFO

Article history:

Received 3 April 2012

Received in revised form

14 May 2012

Accepted 22 May 2012

Available online 12 June 2012

Keywords:

Annexin II
 Pancreatic cancer
 Gemcitabine
 Akt
 mTOR

ABSTRACT

Background: Although gemcitabine has been widely used as a first-line chemo reagent for patients with pancreatic cancer, the response rate remains low. We previously identified Annexin II as a factor involved in gemcitabine resistance against pancreatic cancer. The aims of this study were to elucidate the signaling mechanism by which Annexin II induces gemcitabine resistance and to develop a new therapy that overcomes the resistance against gemcitabine.

Methods: We compared the specific profiles of 12 targeted phosphorylated (*p*-) signaling proteins in gemcitabine-resistant (GEM-) and its wild-type pancreatic cancer cell lines (MIA PaCa-2) using the Bio-Plex assay system. We also evaluated the expression levels of Annexin II and two phosphoproteins, which showed different expressions in these two cell lines, by immunohistochemistry.

Results: Annexin II overexpression was significantly associated with rapid recurrence after gemcitabine-adjuvant chemotherapy in patients with resected pancreatic cancer ($P < 0.05$). Bio-Plex analysis showed up-regulation of *p*-Akt in GEM-MIA PaCa-2 cells in which Annexin II is highly expressed. The expression level of *p*-Akt was significantly correlated with that of the downstream protein, *p*-mTOR, in pancreatic cancer tissues. Inhibition of mTOR phosphorylation canceled gemcitabine resistance in GEM-MIA PaCa-2 cells.

Conclusions: The Akt/mTOR pathway is involved in mechanisms of gemcitabine resistance induced by Annexin II in pancreatic cancer cells. This indicates that combination therapy with the mTOR inhibitor may overcome gemcitabine resistance. Annexin II as an indicator for selection of gemcitabine resistance could thus be applied to the development of novel tailor-made approaches for pancreatic cancer treatment.

© 2012 Elsevier Inc. All rights reserved.

* Corresponding author. Department of General Surgery, Graduate School of Medicine, Chiba University, 1-8-1 Inohana, Chuo-ku, Chiba 260-8670, Japan. Tel.: +81-43-226-2103; fax: +81-43-226-2552.

E-mail address: yoshitomi@faculty.chiba-u.jp (H. Yoshitomi).

0022-4804/\$ – see front matter © 2012 Elsevier Inc. All rights reserved.

doi:10.1016/j.jss.2012.05.065

1. Introduction

Recent advances in pancreatic cancer treatment have improved the prognosis of the disease. However, these improvements have yet to achieve satisfactory efficacy of patients with pancreatic cancer, in whom the 5-y survival rate is <10%. Although surgical resection is the only hope for a cure, the prognosis of the patient remains poor even after curative surgery because of the high recurrence rate [1,2].

Since Burris *et al* [3] showed the efficacy of gemcitabine as a chemotherapeutic reagent for pancreatic cancer, this drug has become first-line therapy for patients with unresectable pancreatic cancer. This new chemotherapy has also been applied to multidisciplinary treatments, combining surgery and chemotherapy. Oettle *et al* [4] indicated that adjuvant chemotherapy using gemcitabine improved disease-free survival in patients with resected pancreatic cancer.

Because the efficacy of gemcitabine is limited, with a response rate of about 5% [3], combinations with other cytotoxic agents or molecular targeting agents have been tested in systematic chemotherapy or the adjuvant therapy setting. To date, only minor or no additional effects have been reported [5,6]. Clarification of the molecular mechanisms of resistance against gemcitabine is needed for the development of a new therapy to overcome this resistance.

We recently reported Annexin II as a gemcitabine-resistant factor by comparing the protein profiling of gemcitabine-resistant (GEM-) and wild type (WT-) MIA PaCa-2 cell lines using two-dimensional gel electrophoresis [7,8]. Immunohistochemistry demonstrated Annexin II expression mainly at the surface of pancreatic cancer cells, as well as an association of its high expression with rapid recurrence after gemcitabine-adjuvant chemotherapy in postoperative patients with pancreatic cancer. We also found that inhibition of Annexin II expression in GEM-MIA PaCa-2 cells significantly increased the chemocytotoxic efficacy of gemcitabine [8]. Therefore, we pursued the role of Annexin II in gemcitabine resistance in pancreatic cancer cells.

Annexins comprise a family of calcium-dependent phospholipid-binding cell surface proteins that have diverse cellular functions, including membrane-cytoskeleton organization, vesicular trafficking, and regulation of ion channel activity [9]. Annexin II was also found to be a chemoresistant factor in human breast cancer [10–12]. Zhang *et al* [12] indicated that Annexin II has a critical role in the invasion and metastasis of Adriamycin-resistant breast cancer cells, and that this ability is associated with multidrug resistance. However, it is unclear how Annexin II induces chemoresistance in cancer cells.

Phosphorylation of multiple signal transduction pathways in cancer cells is crucial for cancer proliferation and survival. Signaling pathways such as extracellular signal-related kinase (ERK) signal and Akt/mammalian target of rapamycin (mTOR) pathways are well known to be involved in pancreatic cancer cell growth [13].

Herein, we tried to determine the signaling pathway involved in gemcitabine resistance by Annexin II using the Bio-Plex phosphorylation protein assay system, and found the Akt/mTOR signaling pathway to be involved in Annexin II-related gemcitabine resistance. We also found that

application of both Annexin II and specific inhibition of the Akt/mTOR pathway may provide novel molecular targets for pancreatic cancer therapy.

2. Materials and methods

2.1. Tissue samples

We obtained formalin-fixed paraffin-embedded tissues from 107 patients with pancreatic cancer who had undergone pancreatectomy at Chiba University Hospital between 2001 and 2009. All patients had been diagnosed histologically with primary invasive pancreatic ductal adenocarcinoma for which surgery was curative. The ethics committee of our institute approved this protocol and we obtained written informed consent from each patient before surgery.

2.2. Immunohistochemistry

We performed immunohistochemical analysis as described previously [8]. We used the following primary antibodies and detected the epitopes using the LSAB+ kit (Dako, Tokyo, Japan): anti-Annexin II polyclonal antibody (Santa Cruz Biotechnology, Inc, Santa Cruz, CA; diluted 1:300), anti-human phospho(*p*)-Akt (Ser473) monoclonal antibody (Cell Signaling Technology, Beverly, MA; diluted 1:50), and anti-human *p*-mTOR (Ser2448) monoclonal antibody (Cell Signaling Technology; diluted 1:50). We scored staining patterns as described previously [8]: low expression = 0%–30% of tumor cells with positive staining, and high expression = >30% of tumor cells with positive staining.

2.3. Cell lines and reagents

We obtained the human pancreatic cancer cell line, MIA PaCa-2 (named WT-MIA PaCa-2 in this study), from American Type Culture Collection (Manassas, VA). We established the gemcitabine-resistant MIA PaCa-2 (GEM-MIA PaCa-2) cell line by exposing gemcitabine to WT-MIA PaCa-2 cells repeatedly, as previously described [7]. We maintained WT- and GEM-MIA PaCa-2 cells as previously described [7], and purchased gemcitabine and rapamycin from Toronto Research Chemicals (Toronto, Canada) and Calbiochem (Darmstadt, Germany), respectively.

2.4. Bio-Plex phosphorylation protein assay system

Phosphoproteins were analyzed using Bio-Plex phosphoprotein array (Bio-Rad, Hercules, CA) based on multiplex sandwich bead immunoassays. We used phosphoprotein determination kits (Bio-Rad) according to the manufacturer's recommendations. We prepared protein extracts using a cell lysis kit (Bio-Rad).

Briefly, we incubated protein extracts overnight in 96-well plates with fluorescent capturing beads coupled to antibodies directed against 12 phosphoproteins (*p*-Akt, *p*-NF- κ Bp65, *p*-ERK1/2, *p*-JNK, *p*-MEK1, *p*-p38MAPK, *p*-CREB, *p*-p70S6kinase, *p*-HSP27, *p*-PDGF receptor- β , *p*-Stat3, and *p*-Stat6) and 8 total

proteins (t-Akt, t-I κ B- α , t-ERK1/2, t-JNK, t-MEK1, t-p38MAPK, t-CREB, and t-HSP27). We washed plates and incubated them with biotinylated antibodies fixing each target protein. We then added streptavidin-phycoerythrin solution. We recorded results as mean fluorescence intensities and compared them with negative controls. We performed all experiments in duplicate, two independent times.

2.5. Western blotting

We purchased anti-t-Akt, anti-p-Akt (Ser473), anti-t-mTOR, and anti-p-mTOR (Ser2448) monoclonal antibodies from Cell Signaling Technology, and anti-Annexin II polyclonal antibody and anti- β -actin antibody from Santa Cruz Biotechnology. We washed subconfluent WT- and GEM-MIA PaCa-2 cells in six-well plates twice with phosphate-buffered saline, lysed them with appropriate lysis buffer, and incubated them after centrifugation, as previously described [8]. We separated the supernatant proteins (20 μ g) by electrophoresis on 10%–20% gradient gels (PerfectNT Gel; DRC, Tokyo, Japan) for t-Akt and p-Akt, and 7.5% gels for t-mTOR and p-mTOR. We transferred these proteins to polyvinylidene fluoride membranes (Millipore, Bedford, MA), and reacted the membranes with anti-t-Akt (diluted 1:1000), anti-p-Akt (diluted 1:2000), anti-t-mTOR (diluted 1:1000), and anti-p-mTOR (diluted 1:1000) for 2 h at

room temperature. We used goat anti-rabbit immunoglobulin G horseradish peroxidase (diluted 1:2000) and rabbit anti-goat immunoglobulin G horseradish peroxidase (Cappel, West Chester, PA; diluted 1:500) in blocking buffer as secondary antibodies. We detected antigens on the membrane using enhanced chemiluminescence detection reagents (Amersham Pharmacia Biotech, Piscataway, NJ). We measured the intensity of each band using NIH image (NIH, Bethesda, MD) and calculated the relative protein levels normalized to that of β -actin.

2.6. Inhibition of Annexin II expression using short interfering RNA (siRNA) in vitro

We performed the specific inhibition of Annexin II expression as described previously [8]. We used siRNA that specifically targeted Annexin II mRNA (Anx2 siRNA) to reduce Annexin II expression. The target sequences for Annexin II RNA interference were composed of a duplex of siRNA: 5'-GUUACAGCCC UUAUGACAUTT-3' and 5'-AUGUCAUAAGGGCUGAACTT-3'. We purchased double-stranded synthetic Anx2 siRNA and luciferase (GL2) siRNA, as a negative control, from Sigma Aldrich (Tokyo, Japan) and Qiagen (Tokyo, Japan), respectively. We performed in vitro transfection using Lipofectamine 2000 reagent (Life Technologies, Carlsbad, CA) according to the manufacturer's instructions.

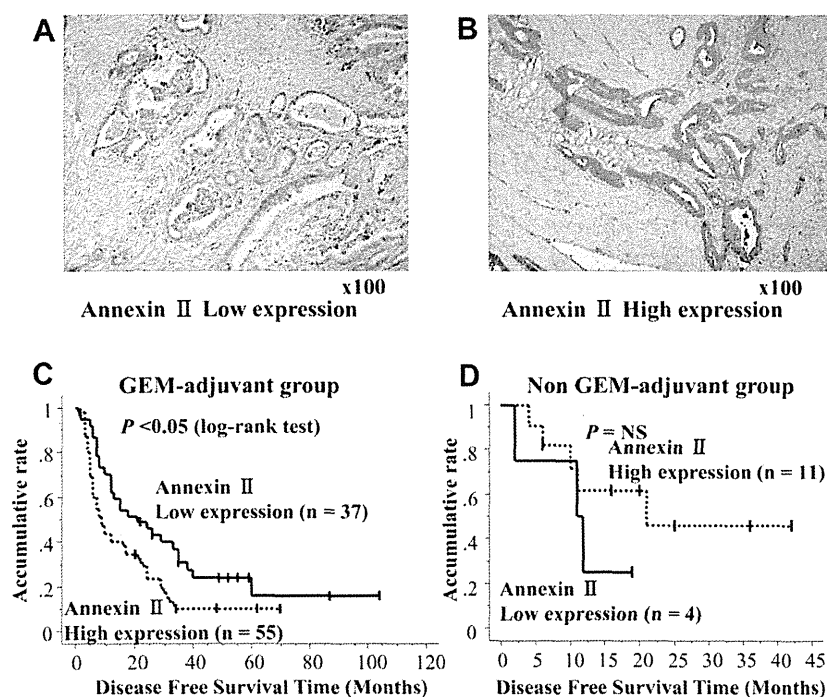


Fig. 1 – Annexin II expression level in pancreatic cancer tissue correlated with disease-free survival after gemcitabine adjuvant chemotherapy. (A, B) Representative findings of Annexin II immunohistochemistry in pancreatic cancer tissues. Microscopic magnification at $\times 100$. Low Annexin II expression (A). High Annexin II expression (B). (C, D) Disease-free survival of patients administered gemcitabine as the adjuvant therapy (GEM-adjuvant group) and those without adjuvant therapy (non GEM-adjuvant group). Disease-free survival was shorter in patients showing a high expression of Annexin II than in those showing a low expression ($P < 0.05$, log-rank test) in the GEM-adjuvant group (C) but not in the non GEM-adjuvant group (D). We estimated disease-free survival using the Kaplan-Meier method and determined the difference between curves using the log-rank test. (Color version of figure is available online.)

Table 1 – Characteristics of 92 pancreatic cancer patients with gemcitabine treatment in IHC analysis.

	Total (92)	Annexin II-IHC staining		P
		Low expression (37)	High expression (55)	
Age (y)	64.8 ± 9.3	64.3 ± 7.7	65.1 ± 10.3	NS
Sex (M/F)	50/42	21/16	29/26	NS
UICC stage				NS
IA	1	0	1	
IB	2	2	0	
IIA	20	10	10	
IIB	64	25	39	
III	2	0	2	
IV	3	0	3	
Resection status				NS
R0	71	27	44	
R1	21	10	11	
Histology				NS
Tubular adenocarcinoma				
Well-differentiated	12	5	7	
Moderately differentiated	56	23	33	
Poorly differentiated	15	6	9	
Papillary	2	1	1	
IPMC (invasive)	4	1	3	
Anaplastic carcinoma	2	1	1	
Adenosquamous carcinoma	1	0	1	

UICC = International Union Against Cancer; NS = not significant; IPMC = intraductal papillary-mutinous carcinoma; R0 = microscopic margin free; R1 = macroscopic margin free.

2.7. Cell cytotoxicity assay

We plated WT- and GEM-MIA PaCa-2 cells at 5×10^3 cells/well in 96-well plates in Dulbecco's modified Eagle's medium containing 10% fetal bovine serum and incubated them for 48 h. For cytotoxicity assay, after we changed the medium with gemcitabine (50 ng/mL) and/or rapamycin (50 nmol/L), we incubated the cells for 72 h. We quantified the number of viable cells by colorimetric cell proliferation assay using the Cell Counting Kit-8 (Dojindo, Kumamoto, Japan) according to the manufacturer's instructions. We performed all experiments in triplicate, four independent times.

2.8. Statistical analysis

We applied Student's t-test for statistical analysis of comparative data. P values <0.05 were considered statistically significant.

3. Results

3.1. Patients with Annexin II overexpression in pancreatic cancer are significantly associated with rapid recurrence

We first examined Annexin II staining of pancreatic cancer tissues by immunohistochemistry to confirm our previous result showing that Annexin II expression level is correlated with gemcitabine efficacy [8]. We performed immunohistochemical analysis on 107 cancer tissues from patients with curatively resected pancreatic cancer. We treated most of these patients (n = 92) with gemcitabine as the adjuvant chemotherapy after operation (GEM-adjuvant); the other 15 patients, including eight who treated with S-1 as the adjuvant therapy, did not receive gemcitabine adjuvant therapy (non

Table 2 – Uni- and Multivariate disease free survival analysis in patients with gemcitabine treatment.

Variables	Univariate analysis			Multivariate analysis		
	Hazard ratio	95% confidence interval	P	Hazard ratio	95% confidence interval	P
Age (>64 y/<= 63 y)	1.201	0.762–1.894	NS			
Sex (F/M)	1.200	0.766–1.879	NS			
Tumor location (Head/body-tail)	0.561	0.328–0.959	<0.05	0.586	0.343–1.001	NS
UICC stage (IA, IB, IIA/IIB, III, IV)	0.434	0.246–0.766	<0.005	0.045	0.006–0.351	<0.005
N (-/+)	0.492	0.282–0.857	<0.05	9.658	1.323–70.482	<0.05
Tumor differentiation (Poorly/well-moderately)	1.595	0.857–2.967	NS			
Annexin II-IHC staining (high/low)	1.787	1.117–2.860	<0.05	1.802	1.121–2.896	<0.05
Resection status (R0/1)	0.775	0.456–1.317	NS			

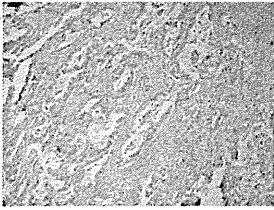
N = lymph node status; R0 = histologically tumor-free surgical margins; R1 = macroscopically tumor-free surgical margins; NS = not significant.

A **Three cases of repeat pancreatectomy after gemcitabine adjuvant chemotherapy**

Case	Age	Sex	DFS after initial operation (months)	Histology (initial / second)	GEM total amount (g)	Annexin II expression (initial / second)
1	68	F	38	IPMC (invasive) / tubular (mod)	91.2	+ / ++
2	76	F	40	tubular (well-mod) / tubular (mod)	13.9	- / +++
3	62	F	29	tubular (mod) / tubular (mod)	79.0	- / ++

DFS, disease free survival; IPMC, intraductal papillary-mucinous carcinoma; tubular, tubular adenocarcinoma; well, well differentiated type; mod, moderately differentiated type; -, no expression; +, weak expression; ++, strong expression; +++, very strong expression.


B



x100

Primary tumor
(initial operation)

C



x100

Recurrence tumor
(after GEM adjuvant chemotherapy)

Fig. 2 – Annexin II expression is increased in recurrent pancreatic cancer after gemcitabine adjuvant chemotherapy. (A) The backgrounds of three patients who underwent repeated pancreatectomy for recurrent cancer in remnant pancreas. Annexin II expression is increased in recurrent cancer tissues compared with that in primary tumor in all three patients. (B, C) Representative images of Annexin II immunohistochemistry in primary (B) and recurrent (C) pancreatic cancer tissues after gemcitabine adjuvant chemotherapy (Case 3 in [A]). (Color version of figure is available online.)

GEM-adjuvant). There were no statistical differences in disease-free and overall survival between patients in GEM-adjuvant and non GEM-adjuvant group (data not shown); this result may have been because of adjuvant therapy with S-1, which showed the same level of anti-tumor effect with gemcitabine [14]. We analyzed Annexin II expression and evaluated it as low or high (Fig. 1A and B). We observe a high level of expression of Annexin II in 55 of 92 patients (59.8%) in the GEM-adjuvant group and 11 of 15 patients (73.3%) in the non GEM-adjuvant group; the Annexin II expression pattern was not significantly different between groups (data not shown).

We next focused on patients treated with gemcitabine as the adjuvant therapy, to analyze whether Annexin II expression level is correlated with the efficacy of this drug. Because many patients in GEM-adjuvant group received other chemotherapy after recurrence, we focused on the disease-free survival of these patients to analyze the efficacy of gemcitabine. Kaplan-Meier analysis showed that a high expression of Annexin II was significantly associated with rapid recurrence ($P < 0.05$, log-rank test) (Fig. 1C). Median disease-free survival was 9 mo for patients characterized with a high expression and 21 mo for those characterized with a low expression of Annexin II. Table 1 lists the characteristics of patients with pancreatic cancer in the GEM-adjuvant group; we found no significant differences in patient background between those in the low and high Annexin II expression groups. Univariate and multivariate analysis showed that the Annexin II expression level was an independent prognostic factor for disease-free survival in these patients (Table 2). In contrast, Kaplan-Meier analysis of patients in the non GEM-adjuvant group revealed no correlation between Annexin II expression level and disease-free survival time (Fig. 1D).

3.2. Annexin II expression is increased in recurrent cancer tissues of patients administered GEM as adjuvant chemotherapy

Of the clinical cases, three patients in the GEM-adjuvant group underwent a second operation for recurrent pancreatic cancer in remnant pancreas after gemcitabine adjuvant chemotherapy. Fig. 2A shows the characteristics and clinical data of these three patients. We analyzed changes in the expression level of Annexin II in situ after long-term use of gemcitabine in these patients. Fig. 2B and C (case 3) shows representative results of Annexin II immunohistochemistry. In the primary tumor resected at the initial operation, we observed weak and faint Annexin II expression, which was increased in the recurrent tumor compared with that in the primary tumor (Fig. 2C). We saw this increase in Annexin II expression in the recurrent tumor in all three patients (Fig. 2A). Thus, Annexin II expression may gradually increase in recurrent cancer tissue under exposure to gemcitabine.

3.3. Akt signal is highly activated in gemcitabine-resistant pancreatic cancer cells

We next investigated the molecular mechanisms of resistance against gemcitabine induced by Annexin II overexpression. We analyzed the signaling pathways up-regulated in the gemcitabine-resistant cell line, which overexpresses Annexin II, compared with the wild-type cell line. Using the Bio-Plex phosphorylation protein assay system, we compared the expression levels of 12 phosphorylated and eight total proteins (see details in Materials and Methods) in WT- and GEM-MIA PaCa-2 cells. Among these proteins, the Akt signal

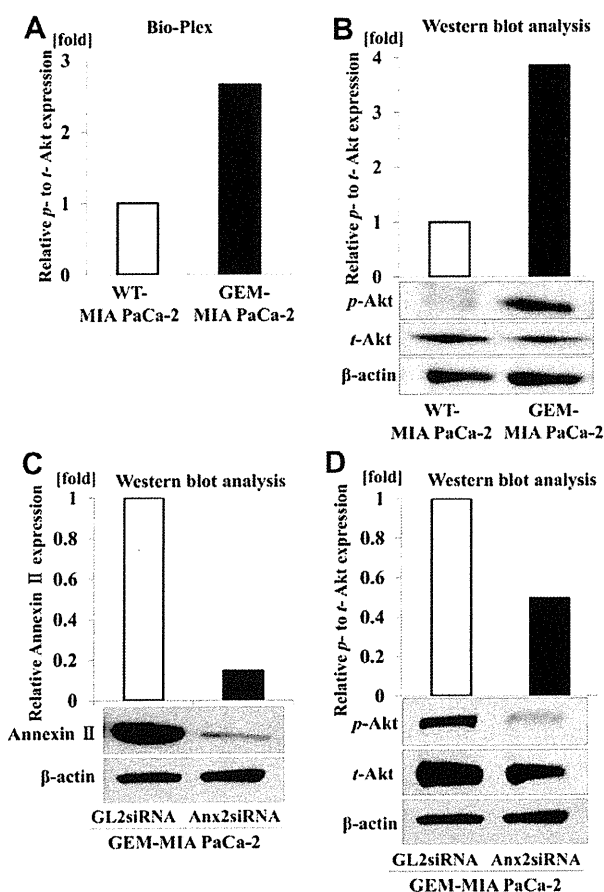


Fig. 3 – Phosphorylation of the Akt signal is up-regulated in gemcitabine-resistant pancreatic cancer cells expressing Annexin II. (A) The relative phosphorylated (*p*)– and total (*t*)–Akt expression is 2.5-fold higher in GEM-MIA PaCa-2 cells than in WT-MIA PaCa-2 cells, as detected by Bio-Plex phosphorylation protein assay analysis. (B) Western blot analysis confirms up-regulation of Akt phosphorylation in GEM-MIA PaCa-2 cells. The relative *p*- and *t*-Akt expression in GEM-MIA PaCa-2 cells is approximately 3.9-fold higher than in WT-MIA PaCa-2 cells. (C) Anx2 siRNA inhibits Annexin II expression in GEM-MIA PaCa-2 cells. Western blot analysis of Annexin II and β -actin in GEM-MIA PaCa-2 cells treated with GL2 siRNA as the negative control or Anx2 siRNA. (D) The relative *p*- and *t*-Akt expression is suppressed in Annexin II-inhibited GEM-MIA PaCa-2 cells. Western blot analysis of *p*- and *t*-Akt, and β -actin as the control, in GEM-MIA PaCa-2 cells treated with GL2 siRNA or Anx2 siRNA. The intensity of each band is measured and the relative protein levels normalized to that of β -actin are calculated (B–D).

was highly activated in GEM-MIA PaCa-2 cells. The relative *p*- to *t*-Akt expression in GEM-MIA PaCa-2 cells was 2.7-fold higher than that in WT-MIA PaCa-2 cells (Fig. 3A). We confirmed this increase in Akt phosphorylation in GEM-MIA PaCa-2 cells by Western blot analysis (Fig. 3B).

Based on these results, we examined whether inhibition of Annexin II expression by siRNA affects Akt signal activation.

Western blot analysis confirmed that Annexin II expression was effectively inhibited by transfection of Anx2 siRNA (Fig. 3C). Gene knockdown by the Anx2 siRNA resulted in the suppression of Akt signal activation (down-regulation of relative *p*- to *t*-Akt expression) in GEM-MIA PaCa-2 cells (Fig. 3D). These results suggest that Annexin II overexpression in gemcitabine-resistant cells is associated with cellular signaling activation of the Akt pathway *in vitro*.

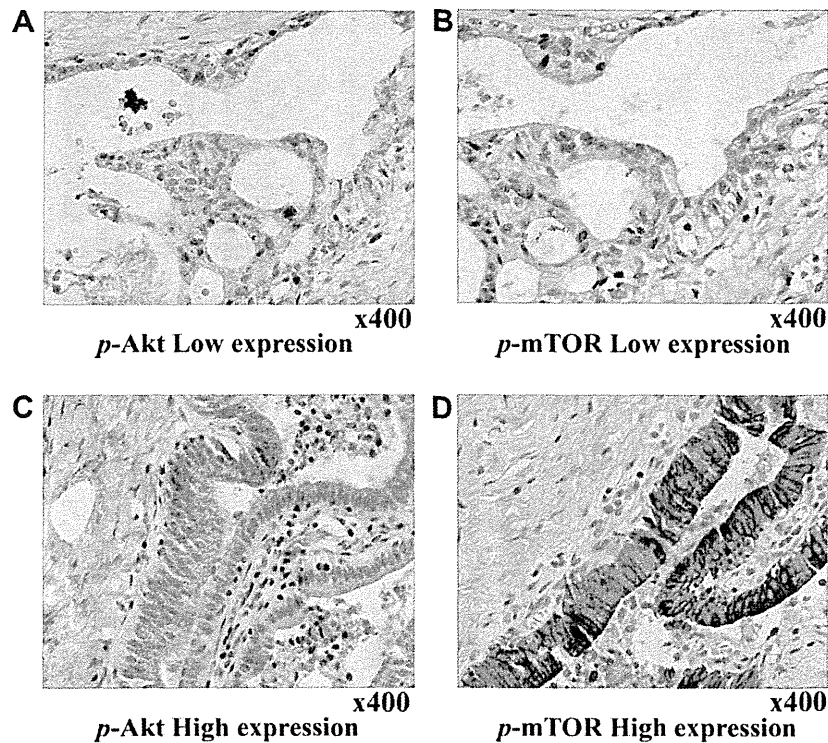
3.4. Phosphorylation levels of Akt and mTOR are significantly correlated in pancreatic cancer tissues

In all 92 patients in the GEM-adjuvant group, we analyzed expression levels of activated Akt and mTOR (*p*-Akt and *p*-mTOR) by immunohistochemistry. We mainly observed expression of both *p*-Akt and *p*-mTOR in the cytoplasm of cancer cells (Fig. 4A–D). We observed strong staining (i.e., high expression) of *p*-Akt and *p*-mTOR in 38 (41.3%) and 43 (46.7%) cases, respectively. Notably, high expression of *p*-Akt was significantly associated with that of *p*-mTOR in serial sections of the same specimen ($P = 0.0005$) (Fig. 4E).

3.5. Inhibition of mTOR activation recovers sensitivity to gemcitabine in GEM-MIA PaCa-2 cells

To confirm whether mTOR activation is correlated with gemcitabine resistance, we treated GEM-MIA PaCa-2 cells with the mTOR inhibitor, rapamycin. We first confirmed gemcitabine resistance in GEM-MIA PaCa-2 cells, which showed less toxicity against gemcitabine compared with WT-MIA PaCa-2 cells. We maximized the difference of this cytotoxicity between GEM- and WT-MIA PaCa-2 cells with 50 ng/mL gemcitabine (Fig. 5A). According to this result, we used gemcitabine with 50 ng/mL concentration in the following examination. We also confirmed the inhibition of m-TOR activation by rapamycin. Western blot analysis of *p*- and *t*-mTOR in WT- and GEM-MIA PaCa-2 cells exposed to rapamycin showed that rapamycin effectively inhibits the activation of mTOR (relative *p*- to *t*-mTOR expression) in both WT- and GEM-MIA PaCa-2 cells (Fig. 5B).

We next examined whether the inhibition of mTOR phosphorylation affects sensitivity to gemcitabine. As shown in Fig. 5A, gemcitabine treatment showed more cytotoxicity in WT- than in GEM-MIA PaCa-2 cells (Fig. 5C, second and sixth columns). Moreover, WT-MIA PaCa-2 cells showed limited cytotoxicity to treatment of rapamycin alone (Fig. 5C, third column) and no additional cytotoxicity to the combined treatment of gemcitabine and rapamycin, compared with cells treated with gemcitabine alone (Fig. 5C, second and fourth columns). Treatment of rapamycin alone showed the same limited cytotoxicity to GEM-MIA PaCa-2 cells as that to WT-MIA PaCa-2 cells (Fig. 5C, third and seventh columns). Interestingly, the combination of rapamycin and gemcitabine showed increased cytotoxicity compared with gemcitabine treatment in GEM-MIA PaCa-2 cells (Fig. 5C, sixth and eighth columns). This additional effect of rapamycin in gemcitabine cytotoxicity reached a maximum at only the 25-nmol/L concentration (Fig. 5D). This cytotoxicity of the combination of rapamycin and gemcitabine in GEM-MIA PaCa-2 cells was almost at same level as that in gemcitabine-treated WT-MIA



E Relationship between *p*-Akt and *p*-mTOR expression.

		<i>p</i> -mTOR		<i>P</i>
		High (n = 43)	Low (n = 49)	
<i>p</i> -Akt	High (n = 38)	26	12	0.0005
	Low (n = 54)	17	37	

Fig. 4 – *p*-Akt and *p*-mTOR expression in pancreatic cancer are well correlated. (A–D) Representative immunohistochemical staining of *p*-Akt and *p*-mTOR in pancreatic cancer tissues. Low expression of *p*-Akt (A) and *p*-mTOR (B). High expression of *p*-Akt (C) and *p*-mTOR (D). Microscopic magnification at $\times 400$. (E) There is a significant correlation between the expression levels of *p*-Akt and *p*-mTOR in pancreatic cancer tissue ($P = 0.0005$). (Color version of figure is available online.)

PaCa-2 cells (Fig. 5C, second and eighth columns), which suggests cancellation of gemcitabine resistance in GEM-MIA PaCa-2 cells by rapamycin.

4. Discussion

Although gemcitabine has led to important progress in pancreatic cancer treatment in the past decade, the efficacy of this reagent is still limited. Thus, elucidation of the mechanisms underlying gemcitabine resistance is important.

Using a proteomic approach, we previously demonstrated that Annexin II is the important factor of gemcitabine resistance. Chuthapisith *et al* [10] showed that Annexin II is involved in chemoresistance to breast cancer. They reported 20 proteins including Annexin II with altered expression in both Adriamycin- and paclitaxel-resistant cells using two-dimensional gel electrophoresis and Matrix Assisted Laser Desorption and Ionization time-of (MALDI-TOF) peptide mass fingerprinting.

They also reported that Annexin II positivity correlated with a poor pathological response of neoadjuvant chemotherapy in large or locally advanced breast cancer [11]. Annexin II was thus thought to induce chemoresistance through interruption of the apoptotic pathway, including p53 [15].

Vishwanatha *et al* [16] first indicated that Annexin II mRNA and protein expression are up-regulated in pancreatic cancer tissues and cell lines. Immunocytochemical analysis of colocalization of Annexin II and proliferating cell nuclear antigen further suggested that Annexin II has a role in pancreatic cancer cell proliferation. In this study, we confirmed through Annexin II immunohistochemical staining of pancreatic cancer tissues that high Annexin II expression is correlated with short disease-free survival for patients who receive gemcitabine adjuvant chemotherapy after surgery. On the other hand, for patients who do not receive gemcitabine adjuvant therapy, we found no correlation between Annexin II expression in cancer cells and disease-free survival. Together with the fact that more than half of patients with non

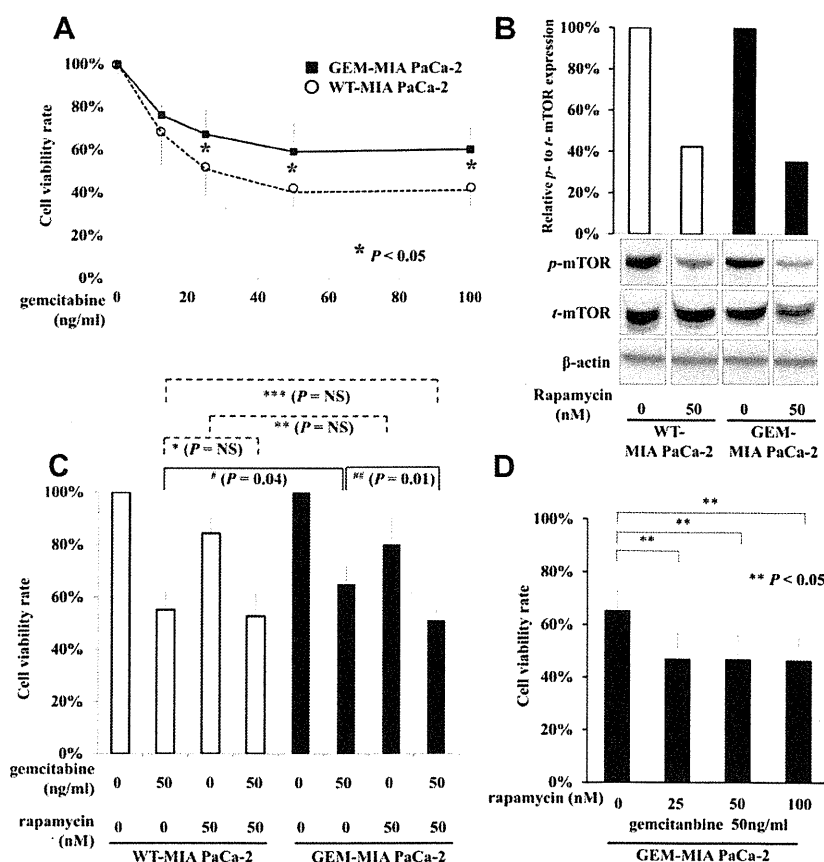


Fig. 5 – Gemcitabine and rapamycin combined therapy recovers gemcitabine sensitivity in GEM-MIA PaCa-2 cells. (A) Gemcitabine is less cytotoxic in GEM-MIA PaCa-2 cells than in WT-MIA PaCa-2 cells. Each point shows the relative number of viable cells treated with gemcitabine in indicated concentrations compared with the number of untreated cells. The asterisk indicates the difference between GEM- and WT-MIA PaCa-2 cells in each gemcitabine concentration. **(B)** mTOR phosphorylation is inhibited by rapamycin in both WT- and GEM-MIA PaCa-2 cells. Western blot analysis of p- and t-mTOR, and β -actin as the control. The intensity of each band is measured and the relative protein levels normalized to that of β -actin are calculated. **(C)** The relative number of viable cells compared with the number of untreated cells. More GEM-MIA PaCa-2 cells survived than WT-MIA PaCa-2 cells treated with 50 ng/mL gemcitabine. Rapamycin treatment cancelled the gemcitabine-resistant state of GEM-MIA PaCa-2 cells, returning to the same levels of WT-MIA PaCa-2 cells. Each column and bar shows the mean \pm SD. NS = not significant. **(D)** Cell toxicity of combination treatment with 50 ng/mL gemcitabine and rapamycin of indicated concentrations in GEM-MIA PaCa-2 cells. Cell viability rate is calculated as relative cell number of each treatment compared with cell number without gemcitabine and rapamycin treatment.

GEM-adjuvant group received S-1 adjuvant therapy, this finding confirms the specific role of Annexin II in gemcitabine resistance to pancreatic cancer.

Ortiz-Zapater *et al* [17] identified that t-PA-related signaling pathways in pancreatic cancer are mediated by epidermal growth factor receptor and Annexin II. This signaling pathway activates the downstream proteins of ERK1/2, which suggests the possibility that Annexin II-related gemcitabine resistance involves proliferative signaling transduction. To elucidate the molecular mechanisms of gemcitabine resistance in pancreatic cancer cells, we investigated the signaling pathways that correlate with Annexin II. We found more activation of the Akt signal in gemcitabine-resistant cells, which strongly express Annexin II, than in wild-type cells. The PI3K/Akt pathway is a major signaling pathway involved in oncogenesis in many types of malignancies. Ng *et al* [18] reported that the

combination of a PI3K inhibitor with gemcitabine may have therapeutic potential in pancreatic cancer cells, and that the PI3K/Akt pathway is constitutively activated in most human pancreatic cancer cell lines [19]. Further evidence suggests that this pathway is activated in pancreatic cancer [20–22].

We revealed that both Akt and its downstream protein, mTOR, are simultaneously activated in pancreatic cancer tissues. mTOR is one of the effectors regulated via the PI3K/Akt pathway and has a central role in cell survival and proliferation [23]. The mTOR inhibitor rapamycin and its structurally related compounds CCI-779, RAD001, and AP23573 are currently in clinical development for use as molecular targeting cancer therapies [24]. Our *in vitro* study showed that the gemcitabine sensitivity of a gemcitabine-resistant cell line, expressing a high level of Annexin II, recovered to the same level as that of the wild-type cell line

using rapamycin, which indicates that the Akt/mTOR pathway is involved in the mechanism of gemcitabine resistance by Annexin II.

This finding is supported by several similar reports that show anti-tumor effects of mTOR inhibitor and gemcitabine combination therapy in pancreatic cancer [25,26]. On the other hand, Wolpin et al [27] reported no clinical benefits of everolimus, another mTOR inhibitor, for patients with advanced, gemcitabine-refractory pancreatic cancer. They considered the insufficient activity of everolimus to result from the presence of a negative feedback loop. That is, inhibition of mTOR leads to an increase in Akt phosphorylation and activation of other Akt target proteins that promote cell survival [28,29]. Our *in vitro* results also suggest insufficient activity of the mTOR inhibitor on pancreatic cancer, because rapamycin alone showed only limited toxicity to both wild-type and gemcitabine-resistant cells. Taken together, our *in vitro* study shows that both gemcitabine and rapamycin in combined therapy may be effective for patients with gemcitabine-resistant pancreatic cancer.

Annexin II could be a good clinical indicator for early recurrence of pancreatic cancer treated with gemcitabine as adjuvant chemotherapy. The Akt-mTOR pathway is involved in the mechanisms of gemcitabine resistance by Annexin II, and mTOR inhibition recovers the sensitivity of resistance. Thus, analysis of the Annexin II expression level in pancreatic cancer tissue may be useful for selecting the chemotherapeutic reagent and may contribute to the establishment of a novel tailor-made therapy for patients with pancreatic cancer. Moreover, combination therapy with the mTOR inhibitor may increase the cell toxic effect of gemcitabine on pancreatic cancer. To confirm this, further clinical prospective studies are needed.

Acknowledgments

This study was supported by a grant from the Ministry of Education, Culture, Science, Sports, and Technology of Japan; the Pancreas Research Foundation of Japan; and a JSGE Grant-in Aid for Scientific Research.

REFERENCES

- [1] Schnelldorfer T, Ware AL, Sarr MG, et al. Long-term survival after pancreatoduodenectomy for pancreatic adenocarcinoma: is cure possible? *Ann Surg* 2008;247:456.
- [2] Katz MH, Wang H, Fleming JB, et al. Long-term survival after multidisciplinary management of resected pancreatic adenocarcinoma. *Ann Surg Oncol* 2009;16:836.
- [3] Burris HA III, Moore MJ, Andersen J, et al. Improvements in survival and clinical benefit with gemcitabine as first-line therapy for patients with advanced pancreas cancer: a randomized trial. *J Clin Oncol* 1997;15:2403.
- [4] Oettle H, Post S, Neuhaus P, et al. Adjuvant chemotherapy with gemcitabine vs observation in patients undergoing curative-intent resection of pancreatic cancer: A randomized controlled trial. *JAMA* 2007;297:267.
- [5] Moore MJ, Goldstein D, Hamm J, et al. Erlotinib plus gemcitabine compared with gemcitabine alone in patients with advanced pancreatic cancer: A phase III trial of the National Cancer Institute of Canada Clinical Trials Group. *J Clin Oncol* 2007;25:1960.
- [6] Yoshitomi H, Togawa A, Kimura F, et al. A randomized phase II trial of adjuvant chemotherapy with uracil/tegafur and gemcitabine versus gemcitabine alone in patients with resected pancreatic cancer. *Cancer* 2008;113:2448.
- [7] Togawa A, Ito H, Kimura F, et al. Establishment of gemcitabine-resistant human pancreatic cancer cells and effect of brefeldin-a on the resistant cell line. *Pancreas* 2003;27:220.
- [8] Takano S, Togawa A, Yoshitomi H, et al. Annexin II overexpression predicts rapid recurrence after surgery in pancreatic cancer patients undergoing gemcitabine-adjuvant chemotherapy. *Ann Surg Oncol* 2008;15:3157.
- [9] Gerke V, Creutz CE, Moss SE. Annexins: linking Ca²⁺ signalling to membrane dynamics. *Nat Rev Mol Cell Biol* 2005;6:449.
- [10] Chuthapisith S, Layfield R, Kerr ID, et al. Proteomic profiling of MCF-7 breast cancer cells with chemoresistance to different types of anti-cancer drugs. *Int J Oncol* 2007;30:1545.
- [11] Chuthapisith S, Bean BE, Cowley G, et al. Annexins in human breast cancer: Possible predictors of pathological response to neoadjuvant chemotherapy. *Eur J Cancer* 2009;45:1274.
- [12] Zhang F, Zhang L, Zhang B, et al. Anxa2 plays a critical role in enhanced invasiveness of the multidrug resistant human breast cancer cells. *J Proteome Res* 2009;8:5041.
- [13] Furukawa T. Molecular targeting therapy for pancreatic cancer: current knowledge and perspectives from bench to bedside. *J Gastroenterol* 2008;43:905.
- [14] Okusaka T, Funakoshi A, Furuse J, et al. A late phase II study of S-1 for metastatic pancreatic cancer. *Cancer Chemother Pharmacol* 2008;61:615.
- [15] Huang Y, Jin Y, Yan CH, et al. Involvement of Annexin A2 in p53 induced apoptosis in lung cancer. *Mol Cell Biochem* 2008;309:117.
- [16] Vishwanatha JK, Chiang Y, Kumble KD, et al. Enhanced expression of annexin II in human pancreatic carcinoma cells and primary pancreatic cancers. *Carcinogenesis* 1993;14:2575.
- [17] Ortiz-Zapater E, Peiró S, Roda O, et al. Tissue plasminogen activator induces pancreatic cancer cell proliferation by a non-catalytic mechanism that requires extracellular signal-regulated kinase 1/2 activation through epidermal growth factor receptor and annexin A2. *Am J Pathol* 2007;170:1573.
- [18] Ng SSW, Tsao MS, Chow S, et al. Inhibition of phosphatidylinositol 3-kinase enhances gemcitabine-induced apoptosis in human pancreatic cancer cells. *Cancer Res* 2000;60:5451.
- [19] Bondar VM, Sweeney-Gotsch B, Andreeff M, et al. Inhibition of the phosphatidylinositol 3'-kinase-AKT pathway induces apoptosis in pancreatic carcinoma cells *in vitro* and *in vivo*. *Mol Cancer Ther* 2002;1:989.
- [20] Schlieman MG, Fahy BN, Ramsamooj R, et al. Incidence, mechanism and prognostic value of activated AKT in pancreas cancer. *Br J Cancer* 2003;89:2110.
- [21] Asano T, Yao Y, Zhu J, Li D, et al. The PI 3-kinase/Akt signaling pathway is activated due to aberrant Pten expression and targets transcription factors NF-kappaB and c-Myc in pancreatic cancer cells. *Oncogene* 2004;23:8571.
- [22] Gong XG, Lv YF, Li XQ, et al. Gemcitabine resistance induced by interaction between alternatively spliced segment of tenascin-C and annexin A2 in pancreatic cancer cells. *Biol Pharm Bull* 2010;33:1261.
- [23] Schmelzle T, Hall MN. TOR, a central controller of cell growth. *Cell* 2000;103:253.

- [24] Vignot S, Faivre S, Aguirre D, et al. mTOR-targeted therapy of cancer with rapamycin derivatives. *Ann Oncol* 2005;16:525.
- [25] Okada T, Sawada T, Kubota K. Rapamycin enhances the anti-tumor effect of gemcitabine in pancreatic cancer cells. *Hepatogastroenterology* 2007;54:2129.
- [26] Ito D, Fujimoto K, Mori T, et al. In vivo antitumor effect of the mTOR inhibitor CCI-779 and gemcitabine in xenograft models of human pancreatic cancer. *Int J Cancer* 2006;118:2337.
- [27] Wolpin BM, Hezel AF, Abrams T, et al. Oral mTOR inhibitor everolimus in patients with gemcitabine-refractory metastatic pancreatic cancer. *J Clin Oncol* 2009;27:193.
- [28] O'Reilly KE, Rojo F, She QB, et al. mTOR inhibition induces upstream receptor tyrosine kinase signaling and activates Akt. *Cancer Res* 2006;66:1500.
- [29] Wan X, Harkavy B, Shen N, et al. Rapamycin induces feedback activation of Akt signaling through an IGF-1R-dependent mechanism. *Oncogene* 2007;26:1932.

Surgical Resection after Downsizing Chemotherapy for Initially Unresectable Locally Advanced Biliary Tract Cancer: A Retrospective Single-center Study

Atsushi Kato, MD, PhD, Hiroaki Shimizu, MD, PhD, Masayuki Ohtsuka, MD, PhD, Hiroyuki Yoshidome, MD, PhD, Hideyuki Yoshitomi, MD, PhD, Katsunori Furukawa, MD, PhD, Dan Takeuchi, MD, PhD, Tsukasa Takayashiki, MD, PhD, Fumio Kimura, MD, PhD, and Masaru Miyazaki, MD, PhD

Department of General Surgery, Chiba University Graduate School of Medicine, Chiba, Japan

ABSTRACT

Background. Surgical resection is the only method for curative treatment of biliary tract cancer (BTC). Recently, an improved efficacy has been revealed in patients with initially unresectable locally advanced BTC to improve the prognosis by the advent of useful cancer chemotherapy. The aim of this study was to evaluate the effect of downsizing chemotherapy in patients with initially unresectable locally advanced BTC.

Methods. Initially unresectable locally advanced cases were defined as those in which therapeutic resection could not be achieved even by proactive surgical resection. Gemcitabine was administered intravenously once a week for 3 weeks followed by 1 week's respite. Patients whose disease responded to chemotherapy were reevaluated to determine whether their tumor was resectable.

Results. Chemotherapy with gemcitabine was provided to 22 patients with initially unresectable locally advanced BTC. Tumor was significantly downsized in nine patients, and surgical resection was performed in 8 (36.4%) of 22 patients. Surgical resection resulted in R0 resection in four patients and R1 resection in four patients. Patients who underwent surgical resection had a significantly longer survival compared with those unable to undergo surgery.

Conclusions. Preoperative chemotherapy enables the downsizing of initially unresectable locally advanced BTC, with radical resection made possible in a certain proportion of patients. Downsizing chemotherapy should be

proactively carried out as a multidisciplinary treatment strategy for patients with initially unresectable locally advanced BTC with the aim of expanding the surgical indication.

Surgical resection is the only method for curative treatment of biliary tract cancer (BTC). This condition has few subjective symptoms in its initial stage, and early diagnosis is difficult despite current advances in diagnostic imaging technology. This means that most cases are discovered at an advanced stage and curative resection is possible in only a limited number of cases, making the prognosis for this disorder extremely bleak.^{1–4} Although cancer chemotherapy has been generally considered as the first-choice treatment for unresectable BTC, BTC has been reported to be highly resistant to antineoplastic treatment until the recent advent of effective chemotherapeutic agents. However, at the start of the 21st century, numerous reports have shown effectiveness of gemcitabine for BTC, and this has become accepted as the standard therapeutic agent for advanced unresectable BTC.^{5–7}

Downsizing chemotherapy and subsequent surgical resection has been already reported as an effective new approach in multidisciplinary therapy for colorectal cancer hepatic metastases and pancreatic cancer.^{8–10} Since the arrival of gemcitabine, an improved efficacy has been revealed in patients with initially unresectable locally advanced BTC to improve the prognosis. Therefore, downsizing chemotherapy and subsequent surgical resection in cases of initially unresectable localized BTC with no distal metastases may be a considerable possible therapeutic new strategy.

To the best of our knowledge, there have been no previous reports of the utility of preoperative downsizing

chemotherapy for BTC, with the present study representing the first. We here report on the feasibility of surgical resection in patients who have undergone downsizing chemotherapy with gemcitabine for initially unresectable locally advanced BTC.

PATIENTS AND METHODS

Determination of Patient Eligibility

This study comprised a retrospective chart review of treatment performed at Chiba University Hospital. All patients underwent pulmonary computed tomography (CT), bone scintigraphy, and positron emission tomography to confirm the absence of distal metastases. Thus, patients with Union for International Cancer Control stage IVB disease was excluded. Each of the cases was discussed in a multidisciplinary setting. Initially unresectable locally advanced cases were defined as those in which surgical resection could not be achieved even by aggressive surgical procedure, including combined vascular resection. In practice, this referred to (1) local invasion of the hepatic artery to be unable to reconstruct; (2) local invasion of the portal vein to be unable to reconstruct; (3) local invasion of the hepatic vein to be unable to reconstruct; (4) extensive infiltration of the bile duct to be unable to achieve a curative resection; and (5) extensive hepatic invasion to be unable to excise due to insufficient remnant liver volume even after portal vein embolization (Table 1). Subjects had Eastern Cooperative Oncology Group performance status values of 0 or 1, no active infection, no major cardiac or cerebrovascular disorders, and no active malignant tumors other than BTC. Patients who had previously undergone chemotherapy and/or radiotherapy to treat BTC were excluded.

In terms of blood biochemistry findings, chemotherapy administration criteria comprised leukocytes $\geq 3,000/\text{mm}^3$, hemoglobin ≥ 9.0 g/l, platelets $\geq 10 \times 10^4$, creatinine ≤ 1.5 g/dl, and total bilirubin, AST, and ALT less than three times the upper limit of normal. Preoperative biliary drainage was performed for patients with obstructive jaundice, and surgery was carried out after serum total bilirubin levels

had dropped to ≤ 3.0 mg/dl. When hepatic resection was required in order to perform curative resection in patients with obstructive jaundice, portal vein embolization was carried out in cases in which the remnant liver volume ratio was $<40\%$, and surgical resection including hepatectomy was performed after the remnant liver volume ratio had reached $\geq 40\%$.¹¹ In patients with normal liver function, portal vein embolization was indicated when the anticipated future remnant liver volume ratio was $<35\%$.

Chemotherapy Schedule and Evaluation of Response

Gemcitabine ($1,000 \text{ mg}/\text{m}^3$) was administered intravenously once a week for 3 weeks followed by 1 week's respite, with a single course comprising 4 weeks. Toxicity was evaluated according to the National Cancer Institute Common Terminology Criteria for adverse events version 3.0. If toxicity of grade 3 or above was observed, administration was immediately discontinued and resumed after recovery to normal values with the gemcitabine dosage reduced to $800 \text{ mg}/\text{m}^3$. If toxicity was still observed, the dose was further reduced to $600 \text{ mg}/\text{m}^3$.¹²

At the end of every two courses of administration, the response was evaluated by enhanced CT on the basis of Response Evaluation Criteria in Solid Tumors (RECIST) group criteria and also evaluated whether tumor was downsized to be sufficient for surgical resection. Patients who were not indicated for surgical resection at that point and who were evaluated as having no change in their tumor continued with gemcitabine administration, whereas those with progressive disease were switched to S-1 (tegafur-gimeracil-oteracil) chemotherapy agents.

Data Analysis

The survival curve was calculated according to the Kaplan–Meier method, and a log rank test was used to test for significant differences. A *P* value of less than 0.05 was regarded as statistically significant.

RESULTS

From January 2004 to December 2010, total 391 patients with BTC were referred to our hospital (Fig. 1). Of these 391 patients, 266 patients underwent laparotomy. Among these 266 patients, 17 patients judged unresectable on the basis of distant metastases in 16 (peritoneal dissemination in ten and distant lymph node metastases in six) and locally advanced disease in one. Thus, 249 patients judged resectable and underwent surgical resection. The other 125 patients were considered unresectable according to preoperative examination (distant metastases in 96 and locally advanced disease in 29). Of these 29 patients with locally

TABLE 1 Definition of initially unresectable locally advanced biliary tract cancer

- Local invasion of the hepatic artery to be unable to reconstruct.
- Local invasion of the portal vein to be unable to reconstruct.
- Local invasion of the hepatic vein to be unable to reconstruct.
- Extensive infiltration of the bile duct to be unable to achieved a curative resection.
- Extensive hepatic invasion to be unable to excise due to insufficient remnant liver volume even after portal vein embolization.

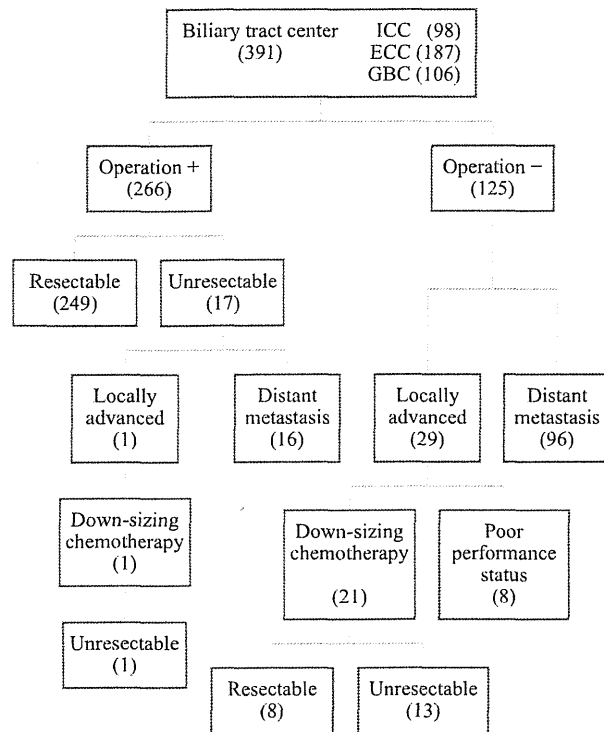


FIG. 1 Treatment schema and outcome for the patients with biliary tract cancer. Numbers in parentheses are numbers of patients. ICC intrahepatic cholangiocarcinoma, ECC extrahepatic cholangiocarcinoma, GBC gallbladder carcinoma

advanced disease, eight could not undergo downsizing chemotherapy as a result of poor performance status. Finally, 22 patients represent the study population with downsizing chemotherapy. Their ages ranged from 57 to 85 years, with an average of 65.3 years, and there were 12 men and 10 women. The final diagnosis was intrahepatic cholangiocarcinoma (ICC) in seven patients, extrahepatic cholangiocarcinoma (ECC) in eight, and gallbladder carcinoma (GBC) in seven (Table 2). Preoperative biliary drainage was performed in 14 (63.6%) of 22 patients with obstructive jaundice, with percutaneous transhepatic biliary drainage in nine cases and endoscopic retrograde biliary drainage in five. Biliary drainage was performed in one of seven patients with ICC, all eight patients with ECC, and five of seven patients with GBC. Chemotherapy was initiated in these patients with obstructive jaundice after serum total bilirubin levels had decreased to ≤ 3.0 mg/dl.

According to our definition of initially unresectable locally advanced BTC, the reason for unresectability was local invasion of the hepatic artery in 18 patients, local invasion of the portal vein in seven, local invasion of the hepatic vein in two, extensive infiltration of the bile duct in three, and insufficient remnant liver volume in two. Ten patients had more than one reason for unresectability.

Three patients (patients 5, 6, and 21) with insufficient remnant liver volume underwent portal vein embolization and started chemotherapy 2 weeks later. Among three patients who underwent portal vein embolization, two patients could undergo surgical resection because the remnant liver volume was sufficient. One patient could not undergo surgical resection because of insufficient remnant liver volume even after portal vein embolization. One patient with insufficient remnant liver volume did not undergo portal vein embolization because of multiple bilobular hepatic metastases in ICC (patient four).

Response was evaluated every two courses, tumor was significantly downsizing in nine patients. On the basis of the RECIST criteria, three patients had a partial response, 11 had stable disease, and eight had progressive disease. Obvious reduction of tumor size, including disappearance of invasion of the hepatic vein and hepatic artery, was seen in eight patients with downsizing tumor, and surgical resection was judged to be feasible in these patients.

Surgical resection was performed in 8 (36.7%) of 22 patients after obtaining tumor downsizing by chemotherapy. Preoperative biliary drainage was performed in 3 (37.5%) of eight patients who underwent surgical resection. The period from the start of chemotherapy to surgery in these eight patients was 5.4 ± 2.3 months (mean \pm standard deviation), and the dose of gemcitabine administered was $21,400 \pm 12,000$ mg (mean \pm standard deviation). Hepatectomy procedures were selected left trisectionectomy in two, left hemihepatectomy with caudate lobectomy in two, right hemihepatectomy with caudate lobectomy in two, and central inferior hepatectomy in two patients. Extrahepatic bile duct resection was performed in seven patients. Combined portal vein resection and inferior vena cava resections were performed in three patients each. After surgery, cholangiojejunal anastomotic failure occurred in one and intraperitoneal abscess in two patients. However, all patients who underwent surgery were discharged from hospital, with a surgical mortality rate of zero (Table 3).

No macroscopic residual tumor (R2) was observed in any of the patients who underwent surgical resection, with four patients classified as R0 and four as R1. Gemcitabine was administered to all patients who underwent surgical resection as postoperative adjuvant chemotherapy. Two of eight patients who underwent surgical resection have now survived for 42 and 13 months, respectively, without recurrence. Although four patients with recurrence died of cancer, two patients with recurrence are still alive after switching to chemotherapy with S-1. The 2 years overall survival rate in patients with surgical resection after downsizing chemotherapy and chemotherapy alone without surgical resection were 45.0 and 19.0%, respectively. Patients who underwent surgery survived significantly longer after the induction of chemotherapy compared with